



1 **FRAME v1.0: Advancing Fire Risk Assessment in Tropical Fragmented**
2 **Forests with a Machine Learning Environment**

3 *Anasuya Barik*^{[1]*}, *Somnath Baidya Roy*^[1]

4 ^[1] *Indian Institute of Technology Delhi, Hauz Khas, New Delhi, India*

5 * *Correspondence to: Anasuya Barik (Anasuya.Barik@cas.iitd.ac.in)*

6 **Abstract.** In this study, we develop a comprehensive Fire Risk Assessment with a Machine Learning Environment
7 (FRAME v1.0) for tropical fragmented forest systems by adding fuel availability and anthropogenic ignition factors
8 to a well-known climate-driven fire hazard assessment model. Our work focuses on the forests of India, a
9 representative example of tropical fragmented forest systems in a densely populated country where fire behavior is
10 complex and influenced strongly by natural and human factors. In this work, we first developed a Fire Danger Rating
11 System (FDRS) based on the Fire Weather Index (FWI) module of the Canadian Forest Fire Danger Rating System
12 (CFFDRS) and machine learning (ML) techniques. The integration of ML techniques increased the FDRS's ability to
13 estimate fire probability by 30-50%. While the FDRS forms the core meteorological component of FRAME v1.0, it
14 does not account for other critical drivers. Hence, we extended this FDRS to a comprehensive fire risk assessment
15 framework by incorporating fuel availability and anthropogenic ignition factors using machine learning predictive
16 algorithms with fire count as the target variable. We observed that the neural network-based model performed best
17 among all algorithms across different forest zones of India. Maximum relevance minimum redundancy analysis
18 revealed spatial heterogeneity in dominant fire drivers, although weather remained a consistently critical factor.
19 FRAME v1.0 provides a scalable operational foundation for fire risk assessment in tropical fragmented forests and
20 demonstrates how machine learning can enhance physically grounded fire danger systems.

21

22 **1 Introduction**

23

24 Forest fires are ecologically important phenomena ((Hutto et al., 2016; Pausas & Keeley, 2019). They regulate
25 nutrient cycling, seed germination, and habitat regeneration (Abedi et al., 2018; Carbutt & Kirkman, 2022; Naveh,
26 1989; Zackrisson et al., 1996). However, in humid tropical forests where natural regeneration is difficult, insufficient
27 recovery rates can pose a threat to forest cover (Scheper et al., 2021). The intensification of climate-related factors is
28 leading to uncontrolled fires in these regions, resulting in not only forest cover reductions and biodiversity loss but
29 also economic losses (Jones et al., 2022; Kalogiannidis et al., 2023; Mohanty & Mithal, 2022; Tyukavina et al., 2022;
30 van Wees et al., 2021; Vancutsem et al., 2021).

31

32 Fire risk in tropical fragmented forests is governed by ecological and socio-environmental dynamics that differ
33 substantially from temperate or boreal systems. Fragmentation leads to more exposed forest edges, which are prone
34 to drier microclimates, increased fuel flammability, and higher ignition likelihood (Silva et al., 2018; Silva-Junior et
35 al., 2022). This pattern has been documented in Amazonian forests (Baidya Roy, 2011; Armenteras et al., 2013;



36 Broadbent et al., 2008). In India's Dalma Wildlife Sanctuary, fragmented patches with higher edge density exhibited
37 significantly greater fire severity, confirming the link between fragmentation and increased fire impacts and slow
38 post-fire recovery in tropical contexts (Chaudhary et al., 2022).

39

40 India is a strong example of a landscape with high forest fragmentation which is characterised by a wide range of
41 climatic and forest types, and intense human–environment interactions. Indian forests also have a large number of
42 uncontrolled fires. The Forest Survey of India (FSI) recorded 2,23,333 forest fires between November 2021 and June
43 2022 and 2,12,249 between November 2022 and June 2023 (MOEFCC and Press information Bureau
44 <https://pib.gov.in/PressReleaseIframePage.aspx?PRID=1946413>). Although generally smaller in size than large
45 wildfires in Australia or the Amazon, these fires collectively affect substantial forested areas. As of 2021, 54.40% of
46 India's forests experience occasional fires, 7.49% contend with moderately frequent fires, and 2.40% experience high
47 incidence levels, accounting for a significant land area of 20,074 sq km (ISFR, 2021). In addition to the fire-conductive
48 weather, various socio-economic and fuel related factors affect the occurrence of fire events in Indian forests (Reddy
49 et al., 2012, 2013). India's fragmented forests are interwoven with agricultural lands, grazing areas, and rapidly
50 expanding settlements (Nagendra et al., 2009; Singh et al., 2016; Tripathi et al., 2010). Practices such as crop-residue
51 burning, shifting cultivation, and informal grazing introduce frequent ignition sources along the forest edges
52 (Kandlikar, 2000; Reddy et al., 2019; Singh et al., 2016). High rural population density and dependence on fire for
53 land management further increase anthropogenic ignitions (Li et al., 2009; Vadrevu et al., 2010). With changes in
54 vegetation and weather patterns induced by climate change, many Indian forests are becoming more susceptible to
55 fires (Barik & Baidya Roy, 2023; Mohanty & Mithal, 2022).

56

57 Despite the importance of fire in such landscapes, India lacks a nationwide operational fire risk assessment system.
58 Many countries rely solely on fire weather-based Fire Danger Rating System (FDRS) to represent fire danger (Amiro
59 et al., 2004; Bedia et al., 2018; Carvalho et al., 2008; Dowdy et al., 2009). An FDRS is a tool in wildfire management
60 which categorizes fire danger on a scale ranging from "Low" to "Extreme," providing a quantitative measure of the
61 risk and potential impact of fires (Stocks et al., 1989; Vasilakos et al., 2007). Such weather-based approaches may
62 be sufficient for regions with uniform land-use patterns or regulated fire management. To cater to complex
63 interactions in fragmented systems like India requires a comprehensive system that integrates weather, fuel, and
64 socio-economic drivers to accurately assess fire 'risk', which integrates hazard, vulnerability, and exposure factors
65 (Bergonse et al., 2022; Erni et al., 2021). Such systematic approaches enable fire management agencies to proactively
66 allocate resources, plan responses, and implement preventive measures based on the anticipated fire risk level (Junior
67 et al., 2022; Jolly et al., 2019; Reddy et al., 2017; Taylor & Alexander, 2006).

68

69 To address this gap, we developed a unified forest fire risk assessment framework called Fire Risk Assessment with
70 a Machine Learning Environment (FRAME v1.0) tailored for tropical fragmented forest systems. The framework
71 builds upon a meteorologically grounded FDRS based on Canadian Forest Fire Danger Rating System (CFFDRS)
72 Fire Weather Index (FWI) system (Wagner, 1987) using ERA5 reanalyses (Hersbach et al., 2020; Muñoz-Sabater et
73 al., 2021) data and satellite-based fire observations for calibration and evaluation. This characterises the fire hazard
74 component of overall risk. The FDRS thresholds were computed by integrating the classic methods with machine
75 learning (ML) techniques to introduce more data-driven decisions in the process and improve the overall reliability



76 of the thresholds (Mitsopoulos & Mallinis, 2017; Satir et al., 2017; Ezugwu et al., 2022; Usama et al., 2019). We then
77 extended this weather-based hazard component by integrating fuel characteristics, topographic controls, and
78 anthropogenic exposure variables within a machine learning-based modeling architecture.

79

80 We then characterised the vulnerability of the forest systems through vegetation and topographic factors. Variables
81 such as Normalized Difference Vegetation Index (NDVI) and Enhanced Vegetation Index (EVI) serve as proxies for
82 fuel availability and are essential in understanding the potential for fire spread and intensity in forest areas (Gabban
83 et al., 2008; Michael et al., 2021). Topographic variables include slope, aspect, and elevation. Steeper slopes can
84 accelerate fire spread, while aspects facing prevailing winds may experience higher fire risk (Holden & Jolly, 2011;
85 Vadrevu et al., 2010). At higher elevation, changes in local climate, intensified land-atmosphere feedback and other
86 factors further impact fire occurrences (Alizadeh et al., 2023). Exposure layers included factors related to human-
87 environment interactions. We used variables such as population density and the percentage of urban and agricultural
88 areas within a grid as exposure layers. As most fragmented forests are in close proximity to urban built-up and
89 agricultural land-use regions, the percentage of these areas within a grid serves as an indicator of human presence
90 and agricultural activity. By integrating these variables into our assessment at a spatial resolution of 25 km grid cells,
91 we aim to gain comprehensive insights into fire risk dynamics across diverse landscapes. As the Indian landscape is
92 diverse in climate and vegetation types, ranging from the cold, dry Himalayas to the tropical and subtropical humid
93 climate of the Western Ghats and North-East, and the drier deciduous vegetation of Central India, the inter-
94 relationships between the intermediate factors can vary from zone to zone. In this study, we have considered five
95 forest zones separately while calculating risk to accommodate region-specific driver interactions.

96

97 Overall, this study advances fire risk assessment in fragmented tropical forests by (1) developing an ML-enhanced
98 fire weather-based hazard system, (2) integrating fuel and anthropogenic drivers within a unified risk framework,
99 and (3) demonstrating spatial heterogeneity in dominant fire controls across diverse forest zones. Although
100 demonstrated for India, the proposed framework is designed to be scalable and transferable to other fragmented
101 tropical landscapes facing similar coupled climate-human pressures. This study not only enhances our understanding
102 of fire dynamics in such ecosystems but also provides a practical tool to identify high-risk areas and support targeted
103 fire management.

104

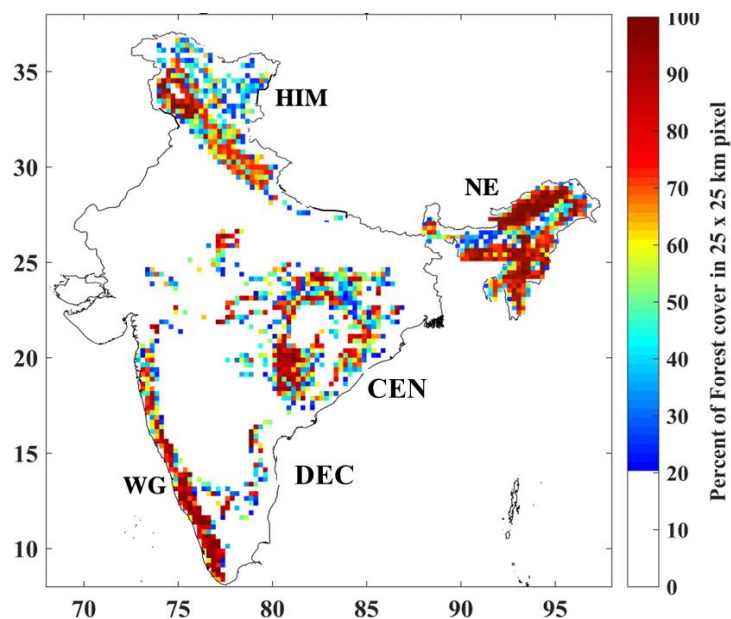
105 **2 Study area**

106

107 India provides a representative example of tropical fragmented forest systems in a densely populated landscape.
108 Forests occupy 27% of the Indian mainland (*India State Forest Report 2021, 2022*). These forests provide a
109 compelling case for studying fire risk in tropical fragmented forests because of high forest fragmentation and diverse
110 climatic and vegetation regimes. To identify the forested regions, we used high-resolution land use land cover data
111 (Roy et al., 2015). The study domain was first divided into 25 × 25 km grid cells. Grid cells with more than 20% of
112 their area classified as any forest type in Roy et al., (2015) were considered forest pixels (Figure 1). Further, we
113 classified these forest pixels into 5 zones as in Barik & Baidya Roy, (2023). These zones are the Himalayan
114 mountainous region (HIM), northeastern India (NE), central India (CEN), the Deccan region (DEC), and the Western



115 Ghats (WG). As the range of FWI varied across these zones, development of the FDRS and risk computation was
116 done separately for each zone.
117



118

119

Figure 1: Study area – forest cover percentages over 5 forest zones of India

120

121 3 Data and Algorithms

122

123 3.1 Meteorological driver data:

124 To represent the weather component of the fire risk assessment system, we use the CFFDRS-FWI, driven by
125 reanalysis-based meteorological data. Specifically, we used the ECMWF's ERA5-Land and ERA5 single-level
126 reanalysis datasets (Hersbach et al., 2020; Muñoz-Sabater et al., 2021). These datasets perform well in India, are
127 extensively used in various applications (Mahto & Mishra, 2019) and provide continuous records from 1981 to the
128 present through the Copernicus Climate Change Service.
129 (<https://cds.climate.copernicus.eu/cdsapp#!/search?type=dataset>). We computed daily maximum 2m Temperature
130 and daily averages of relative humidity, and wind speed from the hourly ERA5 single-level reanalysis dataset at 0.25°
131 resolution. For operational fire danger assessments, the values of these variables at 12 Noon local time are used as
132 the inputs to CFFDRS-FWI. However, for climatological evaluations, daily maximum temperature,
133 average/minimum relative humidity and average wind speed are preferable. Daily averages are less sensitive to short-
134 term fluctuations in weather conditions at specific hours of the day (Purcell, 2003), and they offer a more statistically
135 robust assessment of fire risk over extended periods. In the case of relative humidity, there is a general argument as
136 to whether daily minimum or daily mean is more apt for use in CFFDRS. However, a global study, Quilcaille et al.,
137 (2023) states that using mean or minimum relative humidity would not change the outcomes much. Daily 24-hour



138 accumulated precipitation was obtained from the ERA5-Land dataset at a 0.1° resolution and was regridded to 0.25°
139 resolution.

140

141 **3.2 CFFDRS-FWI:**

142 The fire weather component of the framework was represented using the Fire Weather Index module of the Canadian
143 Forest Fire Danger Rating System, which quantifies the influence of meteorological variables on fuel moisture and
144 potential fire behavior (Stocks et al., 1989; Wagner, 1987). This system originated in Canada and has since become
145 a widely adopted tool for operational fire weather monitoring across the globe (De Jong et al., 2016; Dimitrakopoulos
146 & Papaioannou, 2001; Jolly et al., 2019; Tian et al., 2011). In this study, FWI was computed using ERA5-based
147 meteorological inputs, and regional adjustments developed for Indian climatic conditions were applied following
148 Barik & Baidya Roy, (2023).

149

150 **3.3 Fire data:**

151 To evaluate the performance of the simulated Fire Weather Index (FWI) and to develop the modified fire danger
152 thresholds, we used the Moderate Resolution Imaging Spectroradiometer (MODIS) active fire product (Giglio et al.,
153 2003). This dataset also served as the outcome variable in both the FDRS calibration and the machine learning-based
154 fire risk assessment system. We generated a daily fire frequency dataset at a 25 km resolution from MODIS active
155 fire detections. The MODIS tool on Aqua and Terra satellites detects thermal anomalies at 1km resolution at the time
156 of overpass under relatively cloud-free conditions. This product provides spatially extensive fire occurrence
157 information, making it suitable for evaluating fire weather algorithms and training risk prediction systems. The data
158 is publicly available through NASA's Fire Information for Resource Management System website
159 (<https://firms.modaps.eosdis.nasa.gov/>).

160

161 **3.4 Topography data:**

162 We incorporated topographic information from the Famine Early Warning Systems Network Land Data Assimilation
163 System (FLDAS; McNally et al., 2017; <https://ldas.gsfc.nasa.gov/fldas/elevation>) at 0.1° resolution as part of the fire
164 risk assessment framework. This dataset is derived from a combination of satellite observations and the FLDAS-
165 global surface modelling system. It incorporates input data from NASA's Shuttle Radar Topography Mission (SRTM
166 30m) for elevation with digital elevation models for slope and aspect calculations. These topographical features
167 including slope steepness, elevation gradients, and orientation relative to the sun are used to define the terrain
168 morphology and are important vulnerability layers in fire risk computations. These topographic features affect local
169 microclimates, fuel distribution, and fire spread potential, and are thus important vulnerability layers in the risk
170 assessment.

171

172 **3.5 Vegetation data:**

173 We used the Normalized Difference Vegetation Index (NDVI) and Enhanced Vegetation Index (EVI) derived from
174 the MODIS sensor aboard NASA's Terra and Aqua satellites (Didan & Munoz, 2015);
175 <https://lpdaac.usgs.gov/products/mod13a3v061/>) to characterize vegetation in the risk framework. NDVI and EVI
176 are calculated using reflectance measurements from visible and near-infrared bands, providing valuable insights into
177 vegetation health, density, and phenology. These indices are indicators of vegetation stress, biomass, and fuel



178 availability. Within the fire risk assessment framework, lower values of these indices indicate higher fire vulnerability
179 and exposure in forests.

180

181 **3.6 Population Data:**

182 To represent human exposure to fire risk, we quantifying the population density living within the forest regions. The
183 gridded population dataset from the Socioeconomic Data and Applications Center (SEDAC; Doxsey-Whitfield et al.,
184 2015; <https://sedac.ciesin.columbia.edu/data/collection/gpw-v4/sets/browse>) integrates census data, administrative
185 boundaries, and satellite imagery to estimate population distribution at a global scale at a resolution of 1 km. Utilizing
186 advanced spatial modeling techniques, it provides fine-grained population density information across various
187 geographic regions. We used the annual data for 2003, 2005, 2010, 2015, and 2020 to create an aggregated 25km
188 dataset.

189

190 **3.7 Land Use Land Cover data:**

191 Agricultural and urban land use types are often linked to ignition sources and human activities near forests. To capture
192 this influence in the fire risk framework, we calculated the percentage of land under agriculture and urban use within
193 each 25 km grid. For this, we derived the percentage of land in each 25 km grid under agriculture and urban land use
194 type from the MODIS Land Use Land Cover (LULC). The MCD12Q2 product (Gray et al., 2022;
195 <https://lpdaac.usgs.gov/products/mcd12q2v061/>) is available annually at a 1 km spatial resolution. We used the
196 standard IGBP classes of agriculture/cultivated land and urban built-up areas to compute the percentage datasets at
197 25 km resolution.

198

199 **4 Methods**

200

201 **4.1 Approach**

202

203 The flowchart of the methods used to develop the structured framework to assess forest fire risk is illustrated in Figure
204 2. We begin by computing daily FWI using meteorological inputs from ERA5 data through the CFFDRS system at
205 25 km resolution. Fire observations from MODIS active fire data are used to evaluate the FWI output and generate a
206 gridded forest fire count dataset. This fire count was used to develop the FDRS and as the target variable in the risk
207 model. FDRS thresholds were derived using an ensemble of four statistical approaches integrated with machine
208 learning. This system defined thresholds for fire danger levels to capture the relationship between fire weather and
209 observed fire activity. The resulting FDRS represents the weather-driven hazard component of the FRAME v1.0. To
210 estimate overall fire risk, the hazard component was combined with fuel characteristics (slope, elevation, aspect,
211 NDVI, and EVI) and ignition factors (agriculture, urban area, population density). Seven machine learning algorithms
212 were tested, and an Artificial Neural Network (ANN) was selected based on its predictive performance. The model
213 was trained using 70% of the dataset and validated using the remaining 30%.

214

215 Details of the datasets and modelling steps of FRAME v1.0 framework are described in the following subsections.

216

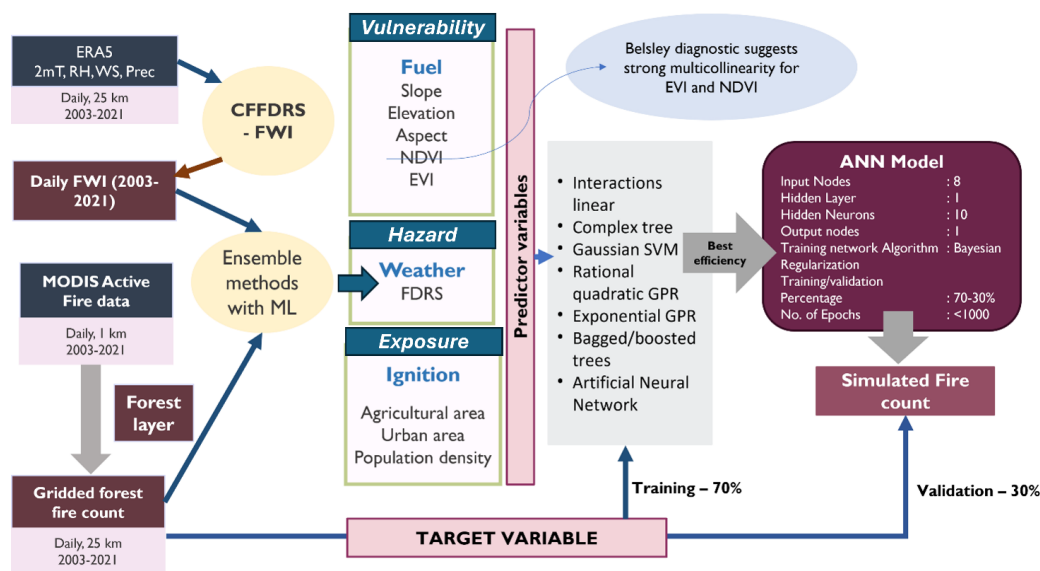


Figure 2: Overview of the FRAME v1.0 framework

217

218

219

220 4.2 Fire frequency dataset development

221

222 We used MODIS active fire data in FRAME v 1.0 for three purposes, as described in detail below. With the fire data,
 223 we evaluated the simulated FWI from CFFDRS, calibrated the FDRS thresholds for each zone, and used them as a
 224 target variable in fire risk assessment. For this, we converted the spatial and temporal information in the active fire
 225 data to a gridded daily fire count dataset at 25 km resolution. To do this, we used the MODIS fire data from January
 226 1, 2003, to December 31, 2021. We then retrieved only those fires occurring in the forest zones of India. This step is
 227 critical, as it removes all fires set in farmlands to burn crop residues to clear the field for the next crop, a practice
 228 widely prevalent in many parts of India. Then, we aggregated the filtered forest fire data into a daily count of fires
 229 within a grid with 25 km spacing, matching the ERA5 weather data and the simulated FWI information. We also
 230 computed zone-wise daily and monthly aggregated climatological fire datasets from this daily fire frequency
 231 information for risk calculations.

232

233 4.3 CFFDRS-FWI configuration

234

235 The CFFDRS calculates the FWI, which is a numerical measure used worldwide by researchers to understand how
 236 weather conditions affect forest fuels and fires, and to study patterns of fire severity (Wagner, 1987). This index
 237 comprises of three moisture codes: the Fine Fuel Moisture Code (FFMC) to quantify surface moisture, the Duff
 238 Moisture Code (DMC) for moisture below the surface, and the Drought Code (DC) for deeper soil levels. It then
 239 calculates two intermediate indices: the Initial Spread Index (ISI) indicating fire spread rate and the Buildup Index
 240 (BUI) indicating available fuel for combustion. The FWI is calculated from ISI and BUI.

241



242 We wrote the code for this algorithm in MATLAB using the equations described in Wagner, (1987)
243 (https://github.com/anasuya993/CFDRS-FWI_India/blob/main/CFDRS_FWI_year_ABitd.m). We then provided
244 gridded (25km) ERA5 meteorological inputs to the algorithm. We implemented the latitude adjustments as in Barik
245 & Baidya Roy (2023) and performed experiments to deduce the spin-up required (Refer to Supplementary Annexure
246 1) and tested the compatibility of the CFDRS with Indian weather (Refer to Supplementary Annexure 2).

247

248 **4.4 Association between FWI and fire frequency**

249

250 To test the association between fire data and the simulated ERA5-based FWI, we used three non-parametric statistical
251 tests as in Barik & Baidya Roy, (2023). These tests include the Chi-square test of association/ independence
252 (McHugh, 2013), Yule's correlation (Yule, 1897), and Fisher's exact test (Upton, 1992). These tests are best applied
253 over nominal or ordinal variables. Hence, we converted the FWI to a nominal variable by introducing data bins. FWI
254 values lesser than the 40th percentile were considered to be zero and the rest values to be 1. We chose this threshold
255 of the 40th percentile based on the observation that the curve of the percentile ranks showed maximum change in
256 slope with 97.9% of fires occurring beyond this threshold. The presence and absence of fire were denoted as 1 and 0
257 respectively.

258

259 In addition, we also plotted the Epanechnikov Kernel Density Estimations (KDE; Epanechnikov, 1969; Samiuddin
260 & El-Sayyad, 1990) to compare the distribution of FWI values corresponding to fire and no-fire events. This approach
261 demonstrated the distinct differences in FWI spread, suggesting that it is an effective metric for identifying conditions
262 conducive to fire occurrence.

263

264 **4.5 Developing FWI thresholds for fire danger classes**

265

266 Fire danger rating is a necessary tool for the quantitative assessment of fire danger in a systematic way (Stocks et al.,
267 1989; Vasilakos et al., 2007). It is a medium to communicate with all stakeholders including the public about potential
268 threats. In FRAME v1.0, we chose five classes Low, Medium, High, Very high, and Extreme because they adequately
269 represent the FWI spread over the zones. To compute the upper FWI thresholds for these danger classes, we selected
270 4 methods from Barik & Baidya Roy, (2023). These 4 methods are based on logistic regression, percentile-based,
271 percentage of fire-based and K-means clustering (Refer to Supplementary Annexure 3). We excluded the geometric
272 progression method in Barik & Baidya Roy, (2023) as it did not include the fire count in the threshold computation.
273 We then introduced machine learning techniques like Receiver Operating Characteristics (ROC) and hierarchical
274 clustering to reduce subjective decision-making in these methods and computed modified thresholds in terms of
275 percentiles. The range of FWIs varied across zones. So, we calculated specific thresholds for each zone.

276

277 We calculated the Critical Success Index (CSI) of the methods against the newly developed thresholds to assess the
278 extent of improvement achieved by including ROC and clustering techniques. More details on the evaluation and
279 robustness check of the developed FDRS thresholds are in Supplementary Annexure 4. The ensemble of the
280 thresholds from all the updated methods formed the FRAME v1.0 FDRS component.

281



282 4.6 Fire risk computation

283

284 The final objective of FRAME v1.0 was to estimate spatial fire risk by integrating the hazard component derived
285 from FDRS with additional vulnerability and exposure indicators. These components were calculated using various
286 predictor layers and machine learning algorithms. The fire weather severity or FDRS rating formed the hazard factor.
287 Exposure factors consisted of population density data, where higher densities indicated increased exposure to fires.
288 Additionally, layers representing agricultural land and urban built-up percentages also served as proxies for exposure.
289 Vulnerability was characterized by fuel condition, for which we used NDVI and EVI as proxies for vegetation health.
290 Lower values of these indices denoted greater fuel availability and hence more fire vulnerability. We initially
291 considered both NDVI and EVI, as there is no consensus amongst existing literature regarding which variable is
292 better suited to represent the state of vegetation over fragmented forest systems of India. Topographical features such
293 as elevation, slope, and aspect are standard variables considered in fire risk assessment studies and they are also
294 considered in this study as vulnerability factors. Together, these variables represent the weather, fuel, terrain, and
295 anthropogenic components incorporated in FRAME v1.0 to capture hazard, vulnerability and exposure conditions
296 influencing fire occurrence.

297

298 After aggregating/ resampling all the input layers at 25 km resolution, we first tested the multicollinearity with the
299 Belsley collinearity diagnostic (Belsley, 1991). It evaluates the degree of collinearity among predictor variables in
300 any regression model. The criteria to denote multicollinearity using the Belsley collinearity diagnostic typically
301 involve examining condition indices (CI) and variance decomposition proportions (VDP) of each variable in the input
302 data. In this study, multicollinearity is considered to be present if CI is greater than 30 and the VPD exceeds the
303 default tolerance of 0.5. NDVI and EVI returned $CI > 30$ and high VPD in CEN and DEC regions where forests are
304 most scattered thus, suggesting strong multicollinearity. We retained EVI as a predictor variable in FRAME v1.0 as
305 EVI showed overall better linear correlation with the fire count than NDVI.

306

307 Next, we normalized all our predictor variables namely FDRS, EVI, elevation, slope, aspect, percentage of cultivated
308 land, percentage of urban built-up area, and population density using standard minimum-maximum method. Then,
309 70% of the predictors, randomly selected, were used to train various machine learning based models to simulate fire
310 count. The simulated fire count is representative of probable fire occurrence and hence proxy to fire risk. We
311 evaluated 7 methods such as interactions linear, complex tree, gaussian support vector machine, rational quadratic
312 GPR, bagged boosted trees and ANN with the remaining 30% of the predictor dataset using parameters like
313 coefficient of determination, RMSE and time taken to train the model. We found that the ANN model outperformed
314 all others, achieving the highest coefficient of determination (R^2) and the shortest training time (Annexure 2: Table
315 S1). Therefore, the ANN model was selected for subsequent fire count simulations. The trained ANN model for every
316 zone was then used to compute simulated probable fire count information from the gridded predictors at monthly
317 scale. These simulations represent the spatially distributed fire risk outputs generated by FRAME v1.0.

318

319 Then, we used a popular method called the Maximum Relevance Minimum Redundancy (MRMR) algorithm to
320 determine the zone wise analysis of dominant factors causing forest fires. The MRMR ranks predictors by
321 maximizing their mutual information with the target fire count (relevance) while minimizing mutual information



322 among the predictors themselves (redundancy), then normalizes these relevance scores as weights. We computed
323 these weights pertaining to each variable in causing changes in the target fire count. The weighted predictors were
324 additively aggregated to compute a risk index which was finally scaled between 0 and 1 to maintain uniformity and
325 give relative risk information in between the zones. This normalized index represents the final fire risk output of
326 FRAME v1.0.

327

328 **5 Results and discussion**

329

330 **5.1 Association between FWI and fires**

331

332 The Chi-square goodness of fit test (Cochran, 1952) shows that the FWI dataset belongs to a normal distribution,
333 whereas the fire occurrence dataset does not. Hence, we cannot assume a normal distribution and use Pearson's
334 correlation coefficient and simple linear regression between the two variables. Hence, we used three non-parametric
335 statistical tests. All three tests demonstrate consistent results, indicating a significant association between FWI and
336 fire occurrences. The Chi-square test of association/ independence test returns a value of 8968.6 which is greater than
337 the critical decisive test value. Thus, the association between the two variables was established at a 95% significance
338 level. For computing Yule's correlation (Q), the concordant cells consist of two favorable scenarios wherein low FWI
339 and high FWI correspond to no fire and fire scenarios respectively. The discordant pair consists of unfavorable
340 outcomes for FWI and fire datasets. Q yields a value of 0.803 indicating a strong positive association. Fisher's exact
341 test over FWI and fire data yields a value of $h=1$ at a 95% significance level and an odds ratio of 9.18 (8.54-9.87).
342 This test also suggests a significant non-random association between the fire occurrence and its corresponding FWI
343 value. The odds ratio of 9.18 suggests that the odds are 9.18 times higher that a fire will occur at low FWI values
344 compared to high FWI.

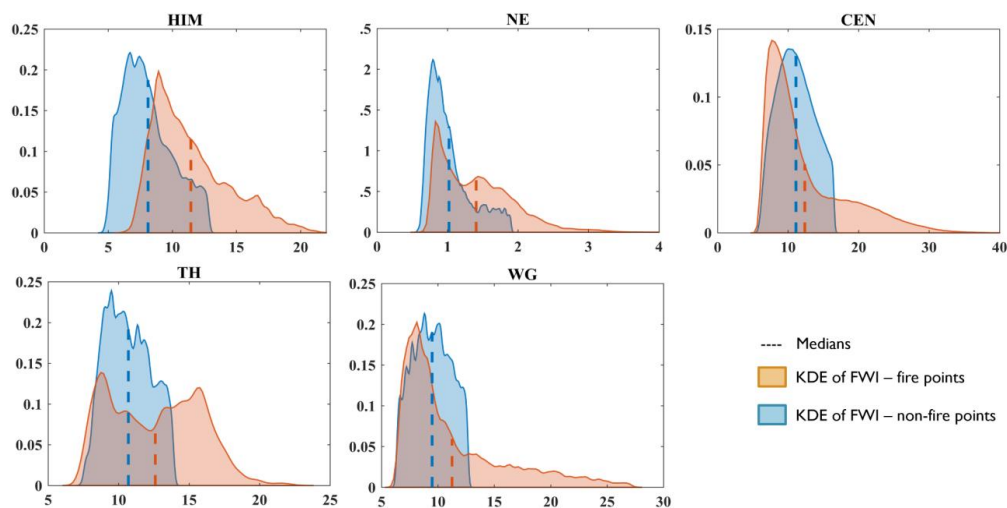
345

346 From the KDE analysis of FWI corresponding to that of fire-occurring grids and no-fire grids (Figure 3), we observed
347 that in all the zones the FWI corresponding to the fire points spread towards higher values. The peak of FWI spread
348 corresponding to no-fire points occurs at comparatively lower FWI values. Also in all the zones, the median of FWI
349 at the fire points curve is at a higher value than that of no-fire points. This confirms that fire occurrences are
350 accompanied by comparatively higher FWIs. The difference between the KDE curves is prominent in HIM, NE and
351 DEC regions. In the CEN and WG regions, although the FWI in fire points extends towards higher values, there is
352 also a notable peak of fire point FWIs at lower values. This can be attributed to the higher fragmentation of forests in
353 these regions, with some grids exhibiting as low as 20-30% forest cover. Consequently, a grid with lower forest cover
354 may exhibit fewer fires compared to a grid with higher forest cover, despite the latter having a lower FWI.

355

356 This demonstrates the strong association of FWI with observed fire counts and hence establishes that the subsequently
357 developed FWI-based FDRS is a strong hazard component for the FRAME v1.0.

358



359

360

Figure 3: Kernel Density Estimation of FWI corresponding to that of fire-occurring grids and non-fire grids for different zones.

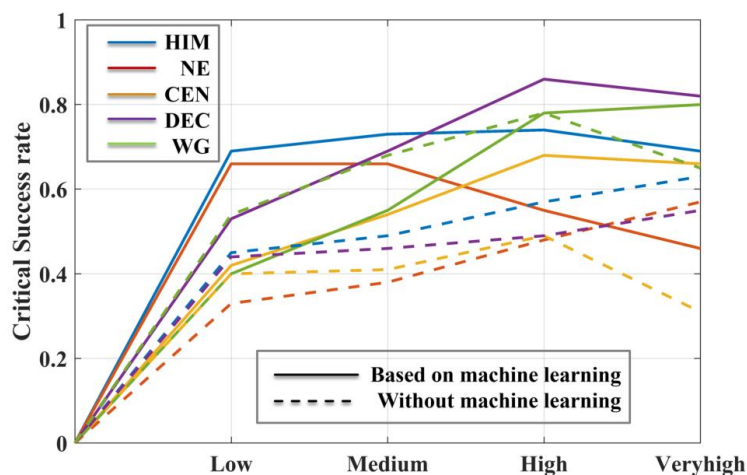
361

362

363 5.2 Evaluation of FDRS

364

365 We calculated the FDRS system threshold in FRAME v1.0 using the methods described in Annexure 3 of the
 366 Supplementary material. The thresholds in (Barik & Baidya Roy, 2023), relying on subjective threshold numbers,
 367 were tailored to specific regions and applications. This limits their usage as potential thresholds for operational usage
 368 for India with all kinds of datasets. To ensure the robustness of these danger classes, we recalibrated the initially
 369 chosen numerical thresholds. The incorporation of clustering and ROC curves provided a more adaptive and data-
 370 driven framework for threshold computation. We used the CSI metric to compare the new thresholds with the
 371 previous ones. CSI is a comprehensive metric that factors in true positives, false positives, and false negatives. The
 372 results show consistently higher CSI values for the thresholds derived from machine learning methods (Figure 4).
 373 This suggests an improvement in the classification to predict fire danger accurately. We observe an overall
 374 improvement of 30-50% in the CSI in all the zones except WG where we observe that Low and Medium class
 375 thresholds show no significant improvement. However, there is a 23% improvement in the CSI of the Very high
 376 danger class. The highest improvement is in the DEC zone followed by CEN with CSI increasing by 49.5% and 43%
 377 respectively in the newer thresholds than the older ones. In the Low and Medium classes, we observe the most
 378 significant improvement in the NE zone. In higher danger classes, DEC and CEN zones show maximum
 379 improvement. In summary, the overall CSI of new thresholds shows an increase of 28% across all classes and zones
 380 in Indian forests. This evaluation shows that the inclusion of objective decision-making approaches significantly
 381 improves the overall performance of the resulting fire danger threshold computation.



382

383 *Figure 4: Critical Success Rate (CSR) of thresholds for each danger class developed without machine*
 384 *learning (dashed lines) and with machine learning (solid lines) for different zones.*

385

386 We developed the upper thresholds for the five fire danger classes in terms of percentiles of FWI (Table 2). Barik &
 387 Baidya Roy, (2023) defined FDRS class thresholds using fixed FWI values specifically for Indian forests and the
 388 datasets and time periods they analyzed. This made those thresholds highly specific to the input data, time period and
 389 region. To ensure that our danger classes remain valid across different tropical zones, and temporal spans, we instead
 390 defined class boundaries in terms of percentiles of the FWI distribution (Table 2). By expressing the thresholds in
 391 terms of percentiles, they become adaptable for use with any dataset, gridded or station data, facilitating a more
 392 versatile and operationally relevant threshold classification. This approach makes the thresholds applicable across
 393 different forest regions, time periods, and FWI datasets, contributing to a robust fire danger assessment framework.
 394 The range of thresholds in terms of percentiles in all the zones is similar with the Low class threshold ranging around
 395 the 40th percentile to the Extreme class beyond the 95th percentile. These percentile thresholds are directly
 396 transferable to other regions with matching the forest and climate characteristics of the 5 zones.

397

398 *Table 2: Upper thresholds of fire danger classes in percentiles of FWI for the different zones*

Fire danger classes	HIM	NE	CEN	DEC	WG
Low	40	36	38	40	34
Medium	61	57	65	66	58
High	85	82	87	90	87
Very high	95	96	97	98	98



Extreme	>95	>96	>97	>98	>98
---------	-----	-----	-----	-----	-----

399

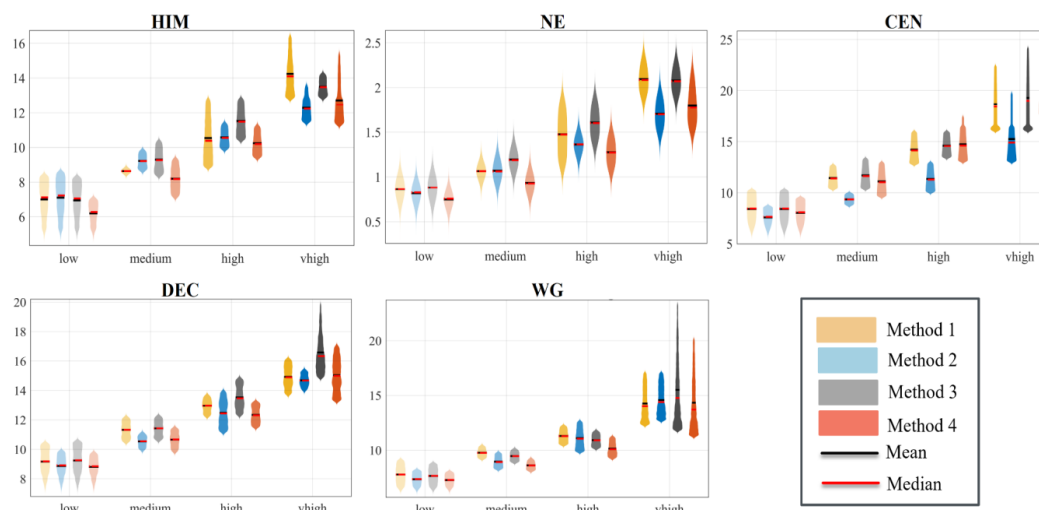
400

401 To ensure the robustness of our developed thresholds, we implemented three key criteria. Firstly, we ensured that
402 there was no overlap between classes when considering different methods. For example, if the low threshold in
403 method 1 surpasses the medium threshold of method 2, then there would be an overlap and it would be inappropriate
404 to use the methods in an ensemble threshold computation. To assess this, we observed the spread of FWI in each
405 class for different methods using a violin plot (Figure 5). This plot combines the aspects of a box plot and a kernel
406 density curve and displays the distribution of data across different categories or groups. The violin shapes convey
407 information about the kernel density of the data in the category, highlighting characteristics such as skewness and
408 multimodality. The black and the red lines indicate the mean and the median of data in that category which provides
409 measures of central tendency.

410

411 From this, we observe that the mean and median thresholds in each method consistently do not overlap with the
412 thresholds of the previous class. This shows agreement between the methods in threshold development, which is
413 essential for their ensemble use. Also, the pattern of kernel densities, including the shape of the kernel density curve,
414 skewness, and relative frequency magnitudes, are in agreement across the chosen methods. This uniformity also
415 shows coherence within the methods and develops confidence in our approach. Another observation is that the spread
416 of kernel densities is more pronounced in the very high class in all the zones. This ensures a broad range of values in
417 the class denoting high fire danger, effectively minimizing the occurrence of true negatives. This strategic emphasis
418 on a comprehensive range in the Very High class enhances the sensitivity of our fire danger thresholds, crucial for
419 accurate risk assessment and management strategies. The observed skewness in the distribution of some methods
420 towards lower values can be attributed to the lower prevalence of highly fire-conducive conditions compared to
421 moderate fire weather conditions. In some zones, the kernel densities in the Low class exhibited skewness towards
422 higher values.

423



424

425 *Figure 5: Violin plots for danger class thresholds developed using logistic regression, percentile-based,*
426 *percentage of fire-based and K-means clustering methods integrated with machine learning, with the*
427 *mean and median marked for different forest zones of India*

428

429 In assessing the second criterion concerning the increasing probability of fire occurrence within each danger class
430 (Figure 6), we computed the probability as the ratio of favorable events—in this case, instances of fire occurrence—
431 to the total number of events in each class. As anticipated, the results show that lower fire danger classes exhibit a
432 correspondingly lower fire probability and the higher fire danger classes demonstrate a higher fire probability. The
433 significance of this probability criterion lies in its role in ensuring the reliability of the established danger classes. If,
434 for instance, a high fire danger class were associated with a low fire probability, it would introduce a contradiction
435 and diminish the practical utility of the thresholds. Therefore, incorporating this probability criterion is essential for
436 developing thresholds that make the delineated danger classes acceptable. Moreover, the violin plot in Figure 5 also
437 illustrates a clear progression of thresholds showing the increase in the spread of FWI values from low to high classes
438 in all the methods. This agreement between fire danger classes and the associated fire occurrence likelihood provides
439 a robust foundation for the developed thresholds.

440

441

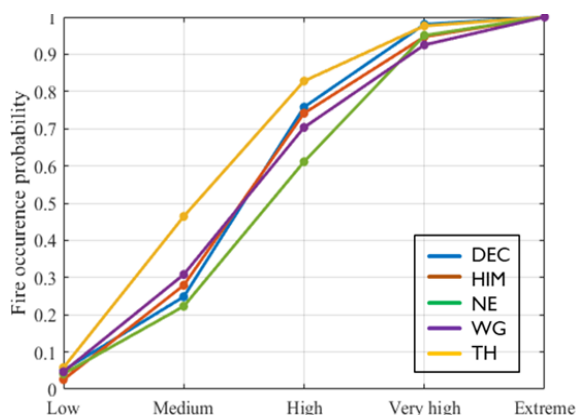


Figure 6: Fire occurrence probability at fire danger classes for different forest zones of India

442

443

444

445

446

447

448

449

450

451

452

453

454

455

456

457

458

459

460

461

462

463

464

465

466

467

468

469

470

Next, in our evaluation of the defined danger classes, we used evaluative parameters to ensure the reliability of the classification. The results reveal a consistently high hit rate across all zones, with the highest value in HIM. This high hit rate indicates the effectiveness of the defined danger classes in capturing true positive events. Hits due to chance are consistently low across all zones. This ensures that the observed hits are not merely coincidental but are due to the model's ability to accurately predict fire occurrences. Correct rejection rates vary within the range of 15-35% across zones, representing the proportion of instances where the model correctly identifies non-fire events. The moderate values in this parameter indicate a balanced classification performance. An interesting observation is the relatively high False Alarm Ratio (FAR), especially in CEN, DEC, and WG zones. This metric is the ratio of false alarms to the total positive predictions. Within these zones, the prevalence of hot and dry conditions during the pre-summer monsoon months contributes to a large number of days having high FWI. However, the presence of high FWI does not necessarily result in fires unless there is an ignition source. This behaviour reflects the conceptual design of FRAME v1.0, where the weather-driven hazard component alone does not determine fire occurrence and must interact with vulnerability and exposure factors to produce actual fire risk.

Despite the elevated FAR in these zones, the overall classification remains acceptable as it does not compromise the accurate identification of true negatives. The comprehensive CSI combines various performance measures and indicates high values in HIM and NE. In other zones, the CSI is comparatively lower because of high false alarms. In summary, the defined danger classes demonstrate coherent values for evaluative parameters, with a consistently high hit rate, low hits due to chance, moderate correct rejections, and an acceptable FAR. This evaluation confirms that the FDRS thresholds provide a robust hazard representation within FRAME v1.0 and can therefore be reliably used as the weather-driven input for the subsequent fire risk modelling framework. The rigorous evaluation of these thresholds makes the designed danger classes suitable for operational fire management use.



471 *Table 3: Evaluative parameters to test the skill of the developed system in fire prediction*

	HIM	NE	CEN	DEC	WG
Critical success rate (CSR)	0.52	0.56	0.26	0.22	0.18
Probability of detection/ hit rate	0.92	0.76	0.56	0.7	0.56
False alarm ratio (FAR)	0.45	0.31	0.67	0.75	0.78
Hits due to chance	0.22	0.36	0.23	0.12	0.13
Correct rejection	0.25	0.15	0.24	0.32	0.33

472

473 **5.3 Evaluation of risk assessment**

474

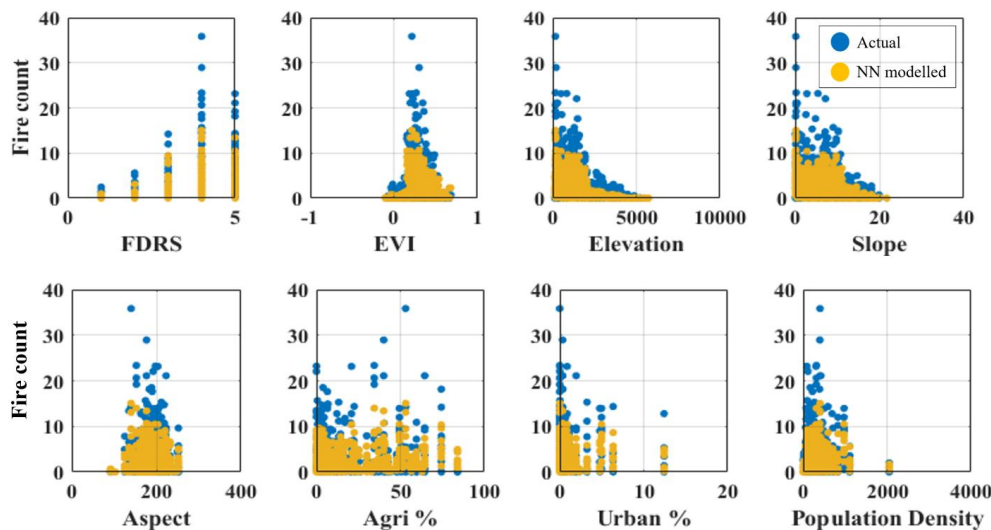
475 Out of all the models used in the study, we found that the ANN model performed the best with least training time and
 476 maximum coefficient of determination that is R^2 values - up to 0.89 in the CEN zone and an average R^2 of 0.73 across
 477 all zones - while maintaining competitive RMSEs (Annexure 2: Table S1). The performance of the ANN model to
 478 capture nonlinear interactions made it the most robust performer among the seven tested methods. The final ANN
 479 architecture, which was selected to be the risk assessment tool in FRAME v1.0, comprised of eight input nodes (one
 480 for each predictor), a single hidden layer with ten neurons, and one output node for fire count. We trained the network
 481 using Bayesian regularization, with a 70 %–30 % train/validation split and under 1,000 epochs.

482

483 Figure 7 shows the simulated and actual fire counts against every predictor variable. Overall, the simulated counts
 484 closely mirror the observed ones, confirming the model’s ability to capture fire occurrence signals. We observe that
 485 higher FDRS values indicate elevated fire hazard thus demonstrating a direct relationship between FDRS and fire
 486 occurrence. The vulnerability layers consist of topographical features like elevation, slope, and aspect. Steeper slopes
 487 and certain aspects may exacerbate fire spread. Higher elevations influence the temperature and fuel moisture
 488 conditions. In addition to these the vulnerability layers also contain indicators such as EVI from which we obtain the
 489 fuel availability information. Lower EVI values suggest dryer vegetation and increase in fire vulnerability. Increase
 490 in agricultural activities and urban built-up area and population increases the chances of human ignition while
 491 agricultural activities may also lead to landscape modifications affecting fire behavior. Overall, the simulated fire
 492 counts match well with the actual fire counts. It is important to note here, the simulated target variable is not an
 493 indicator of absolute fire count per say. Rather a high simulated fire count denotes a higher probability of fire
 494 occurrence.



495



496 *Figure 7: Evaluation of actual and NN simulated fire counts against all the hazard, vulnerability and*
 497 *exposure factors*

498

499 **5.4 Drivers of fire risk**

500

501 Figure 8(a) shows the relative contribution of individual predictor variables in simulating the target fire variable. The
 502 red and the blue dots denote positive and negative relationships between the predictor variable and the target
 503 respectively. It is clear from the figure that FDRS has a positive relationship with fires in all the zones. The relative
 504 importance of this variable is also more than the other variables.

505

506 In the mountainous regions of the HIM, elevation plays the most important role (Figure 8a). With increasing
 507 elevation, the fire susceptibility reduces. This is followed by equal contribution from meteorological and fuel
 508 availability factors. The exposure factors also contribute positively to the overall fire risk in this region. In NE and
 509 CEN, FDRS is the most important governing fire risk. The risk is also prominently higher in the central and southern
 510 NE. The contribution of percentage of urban built-up area is high though the nature of this relationship is less
 511 significant. However, weather and a high built-up area is primarily the reason for higher fire risk in this zone. In CEN,
 512 weather hazard, urban area percentage and population density increases the fire risk. Elevation and EVI factors
 513 counter this, because of which the overall risk is relatively low in the CEN region (Figure 8b). In the DEC region,
 514 fire risk increases with variations in slope and aspect of the landscape. The fuel availability contributes negatively,
 515 and FDRS contributes positively but with low statistical significance. Human influence factors particularly do not
 516 contribute positively to the fire risk in this region. In WG, all the risk factors contribute positively to increasing fire
 517 risk. Fire weather hazard, elevation, and agricultural land percentage are the major reasons behind the fire risk in
 518 western ghat.

519

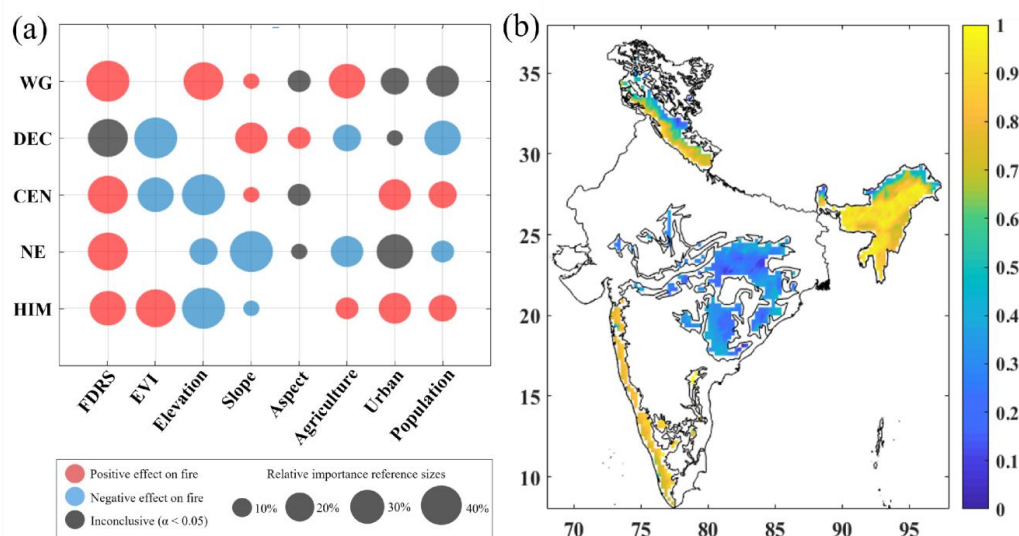


520 Overall, fire weather hazard is the most important factor contributing positively to fire risk in all regions. Another
 521 interesting thing to note is that regions where the urban built-up area contributes positively to the overall fire risk,
 522 population also contributes in similar direction to the fire risk. For example, in CEN and HIM, more built-up area
 523 within the forest zones translates to more population density and hence increased exposure of these regions to forest
 524 fires.

525

526 Figure 8 (b) shows the final, normalized fire risk index as computed by FRAME v1.0 across India, combining weather
 527 hazard, fuel conditions, topography, and ignition factors. High-risk values (>0.8) cluster in the Northeast, where
 528 shifting-cultivation (jhum) burns (Heinimann et al., 2017) and pre-monsoon humidity drops combine to dry fuels
 529 rapidly and sustain frequent ignitions. These regions also have steep slopes and south-facing aspects that dry fuels
 530 quickly. Dense human settlements and agricultural edges further raise ignition probability. The Western Ghats also
 531 show high risk, as semi-evergreen and semi-deciduous forests experience dry pre-monsoon conditions along with
 532 recurring land-clearing burns and accidental ignitions (Renard et al., 2012). Moderate risk (0.4–0.8) spans forests in
 533 the CEN zone, where mixed fuel loads and variable rainfall create intermittent fire windows. In these areas, fuel
 534 continuity is broken by patches of open land. Low risk (<0.4) is found in wet evergreen and high-altitude zones,
 535 where persistent moisture, thick canopy cover, and limited human access keep fuels damp and ignition sources rare.
 536 The fire risk map matches well with the spatial patterns of actual fire occurrence over these zones. This spatially
 537 explicit risk map shows how local climate regimes, terrain morphology, vegetation type, and socio-economic
 538 practices jointly drive fire risk.

539



540

541 *Figure 8: (a) Contribution of individual variables calculated by maximum relevance minimum redundancy*
 542 *algorithm and (b) overall relative fire-risk in FRAME v1.0 over Indian forests*

543

544



545 **6 Conclusion**

546

547 This study presents a comprehensive fire risk assessment framework, FRAME v1.0, tailored for tropical fragmented
548 forest systems, using India as a representative case. We analyzed the complex interplay of biophysical, climatic, and
549 anthropogenic factors in tropical landscapes. As the first step to developing the FRAME v1.0, we developed an
550 adaptable FDRS framework using the CFFDRS. The framework integrates region-specific fire-weather thresholds
551 and uses machine learning to refine thresholds and reduce subjectivity in the fire weather hazard computation. The
552 integration of machine learning techniques, such as ROC curves and clustering, increased the reliability of developed
553 fire danger thresholds for better forest fire prediction and management practices. The developed FDRS framework
554 can independently serve as a reliable indicator of fire weather hazard, helping to understand how weather and climate
555 variables interact to create fire-conducive conditions. However, focusing only on weather-driven hazards provides an
556 incomplete representation of fire risk. Effective fire management requires understanding not only where fires are
557 likely to ignite, but also where ignition is most likely to occur. The integrated risk in FRAME v1.0 identifies areas
558 where high fire hazard coincides with high vulnerability or exposure, highlighting truly high-risk zones. So, we
559 developed the comprehensive FRAME by integrating hazard with key vulnerability and exposure factors, enabling
560 spatially explicit assessment of relative fire risk across tropical fragmented forest systems. We employed ANN to
561 model fire occurrence based on gridded environmental and socio-economic predictors and used the Maximum
562 Relevance Minimum Redundancy (MRMR) algorithm to identify dominant drivers of fire risk across zones. The
563 resulting FRAME v1.0 fire risk index integrates hazard, vulnerability, and exposure dimensions in a scalable manner,
564 which enables comparisons within and across tropical forest regions.

565

566 While FRAME v1.0 was applied in the Indian context in this study, its structure and methodological design are
567 transferable to other tropical forest regions facing similar fragmentation and climate pressures. Gridded assessments
568 such as ours provide a valuable tool for strategic fire management, particularly in data-scarce environments. However,
569 we acknowledge that finer-scale applications would benefit from incorporating additional socio-economic and
570 ecological variables, including detailed fuel composition and localized ignition sources.

571

572 A key methodological advancement is the development of a risk framework that integrates hazard, vulnerability, and
573 exposure into a single, spatially explicit index. We created a workflow that combines FDRS outputs, fuel and
574 socio-economic layers, and machine learning weights in one reproducible pipeline. In addition, the zone-specific
575 calibration of the FDRS builds distinct fire-danger models for each forest zone to account for local climate regimes
576 and vegetation types, unlike one-size-fits-all systems that apply uniform thresholds across diverse landscapes. By
577 coding this end-to-end process, we provide a clear, transferable method for generating comprehensive fire risk maps
578 in tropical fragmented forests.

579

580 Scientifically, these results reveal that fire risk in tropical fragmented forests is controlled by a shifting hierarchy of
581 drivers rather than a single dominant factor. Across all areas, fire weather hazard sets the baseline risk. In mountain
582 zones, higher elevation reduces risk by keeping fuels cooler and moister. In plains and fragmented forests, human
583 factors increase chances of ignition. Fuel availability and terrain shape risk in between. By using machine learning



584 to weigh these zone-specific drivers, we demonstrate that accurate fire risk prediction needs models tailored to local
585 climate, landscape, and human influences.

586

587 Ultimately, this study contributes to the evolving global discourse on fire risk in tropical forest systems by combining
588 operational hazard indicators with machine learning-based risk estimation. FRAME v1.0 provides a foundational
589 step toward scalable and data-driven fire management strategies that can be adapted to similar regions globally,
590 particularly under the increasing pressures of climate change and land use transformations.

591 **7 Author contributions**

592 A.B. and S.B.R. conceptualized the study and designed the overall methodological framework. A.B. developed the
593 analysis workflow, implemented the model framework, and performed the data analysis and simulations. S.B.R.
594 supervised the research and provided guidance on methodology and interpretation of results. A.B. prepared the
595 original manuscript draft. S.B.R. reviewed and edited the manuscript. Both authors contributed to the discussion of
596 results and approved the final manuscript.

597 **8 Competing interests**

598 The authors declare no competing interests.

599 **9 Acknowledgements**

600 The authors acknowledge the Indian Institute of Technology Delhi, India for providing the computational and other
601 infrastructure to conduct this study.

602 **10 Financial support**

603 This research is not funded.

604

605 **11 Data availability**

606 The datasets used in this study are available from the authors upon reasonable request.

607

608 **12 Code availability**

609 The modifiable MATLAB code used to compute the Fire Weather Index is available on the GitHub repository
610 (https://github.com/anasuya993/CFDERS-FWI_India/blob/main/CFDERS_FWI_year_ABiitd.m), and the frozen
611 version 1 is archived on Zenodo (<https://doi.org/10.5281/zenodo.10047237>). The code used for the neural network
612 modelling and fire risk simulations can be made available from the authors upon reasonable request.

613

614

615



616 **11 References:**

- 617 Abedi, M., Zaki, E., Erfanzadeh, R., & Naqinezhad, A. (2018). Germination patterns of the scrublands in response
618 to smoke: The role of functional groups and the effect of smoke treatment method. *South African Journal of*
619 *Botany*, 115. <https://doi.org/10.1016/j.sajb.2017.03.010>
- 620 Alizadeh, M. R., Abatzoglou, J. T., Adamowski, J., Modaresi Rad, A., AghaKouchak, A., Pausata, F. S. R., &
621 Sadegh, M. (2023). Elevation-dependent intensification of fire danger in the western United States. *Nature*
622 *Communications*, 14(1). <https://doi.org/10.1038/s41467-023-37311-4>
- 623 Amiro, B. D., Logan, K. A., Wotton, B. M., Flannigan, M. D., Todd, J. B., Stocks, B. J., & Martell, D. L. (2004).
624 Fire weather index system components for large fires in the Canadian boreal forest. *International Journal of*
625 *Wildland Fire*, 13(4), 391–400.
- 626 Armenteras, D., González, T. M., & Retana, J. (2013). Forest fragmentation and edge influence on fire occurrence
627 and intensity under different management types in Amazon forests. *Biological Conservation*, 159.
628 <https://doi.org/10.1016/j.biocon.2012.10.026>
- 629 Barik, A., & Baidya Roy, S. (2023). Climate change strongly affects future fire weather danger in Indian forests.
630 *Communications Earth and Environment*, 4(1). <https://doi.org/10.1038/s43247-023-01112-w>
- 631 Bedia, J., Golding, N., Casanueva, A., Iturbide, M., Buontempo, C., & Gutiérrez, J. M. (2018). Seasonal predictions
632 of Fire Weather Index: Paving the way for their operational applicability in Mediterranean Europe. *Climate*
633 *Services*, 9. <https://doi.org/10.1016/j.cliser.2017.04.001>
- 634 Belsley, D. A. (1991). A Guide to using the collinearity diagnostics. *Computer Science in Economics and*
635 *Management*, 4(1). <https://doi.org/10.1007/BF00426854>
- 636 Bergonse, R., Oliveira, S., Zêzere, J. L., Moreira, F., Ribeiro, P. F., Leal, M., & Lima e Santos, J. M. (2022).
637 Biophysical controls over fire regime properties in Central Portugal. *Science of the Total Environment*, 810.
638 <https://doi.org/10.1016/j.scitotenv.2021.152314>
- 639 Broadbent, E. N., Asner, G. P., Keller, M., Knapp, D. E., Oliveira, P. J. C., & Silva, J. N. (2008). Forest
640 fragmentation and edge effects from deforestation and selective logging in the Brazilian Amazon. *Biological*
641 *Conservation*, 141(7). <https://doi.org/10.1016/j.biocon.2008.04.024>
- 642 Carbutt, C., & Kirkman, K. (2022). Ecological Grassland Restoration—A South African Perspective. In *Land* (Vol.
643 11, Number 4). <https://doi.org/10.3390/land11040575>
- 644 Carvalho, A., Flannigan, M. D., Logan, K., Miranda, A. I., & Borrego, C. (2008). Fire activity in Portugal and its
645 relationship to weather and the Canadian Fire Weather Index System. *International Journal of Wildland Fire*,
646 17(3). <https://doi.org/10.1071/WF07014>
- 647 Chaudhary, S. K., Pandey, A. C., Parida, B. R., & Gupta, S. K. (2022). Using geoinformatics to link forest fire
648 severity and fragmentation in India's Dalma Wildlife Sanctuary. *Tropical Ecology*, 63(3).
649 <https://doi.org/10.1007/s42965-021-00202-0>
- 650 Cochran, W. G. (1952). The χ^2 Test of Goodness of Fit. *The Annals of Mathematical Statistics*, 23(3), 315–345.
651 <http://www.jstor.org/stable/2236678>
- 652 De Jong, M. C., Wooster, M. J., Kitchen, K., Manley, C., Gazzard, R., & McCall, F. F. (2016). Calibration and
653 evaluation of the Canadian Forest Fire Weather Index (FWI) System for improved wildland fire danger rating
654 in the United Kingdom. *Natural Hazards and Earth System Sciences*, 16(5). [https://doi.org/10.5194/nhess-16-](https://doi.org/10.5194/nhess-16-1217-2016)
655 1217-2016
- 656 Didan, K., & Barreto Munoz, A. (n.d.). *MODIS Vegetation Index User's Guide (MOD13 Series)*. Retrieved May 5,
657 2025, from <https://vip.arizona.edu>
- 658 Dimitrakopoulos, A. P., & Papaioannou, K. K. (2001). Flammability assessment of Mediterranean forest fuels. *Fire*
659 *Technology*, 37(2), 143–152.
- 660 Dowdy, A. J., Mills, G. A., Finkele, K., & Groot, W. De. (2009). *Australian fire weather as represented by the*
661 *McArthur forest fire danger index and the Canadian forest fire weather index (p. 91)*. Centre for Australian
662 Weather and Climate Research.
- 663 Doxsey-Whitfield, E., MacManus, K., Adamo, S. B., Pistolesi, L., Squires, J., Borkovska, O., & Baptista, S. R.
664 (2015). Taking Advantage of the Improved Availability of Census Data: A First Look at the Gridded
665 Population of the World, Version 4. *Papers in Applied Geography*, 1(3).
666 <https://doi.org/10.1080/23754931.2015.1014272>



- 667 Epanechnikov, V. (1969). Nonparametric estimation of a multidimensional probability density. *Teoriya*
668 *Veroyatnostei i Ee Primeneniya*, 14(1), 156–161.
- 669 Erni, S., Johnston, L., Boulanger, Y., Manka, F., Bernier, P., Eddy, B., Christianson, A., Swystun, T., & Gauthier,
670 S. (2021). Exposure of the canadian wildland–human interface and population to wildland fire, under current
671 and future climate conditions. *Canadian Journal of Forest Research*, 51(9). <https://doi.org/10.1139/cjfr-2020-0422>
- 672
- 673 Gabban, A., San-Miguel-Ayanz, J., & Viegas, D. X. (2008). A comparative analysis of the use of NOAA-AVHRR
674 NDVI and FWI data for forest fire risk assessment. *International Journal of Remote Sensing*, 29(19).
675 <https://doi.org/10.1080/01431160801958397>
- 676 Giglio, L., Descloitres, J., Justice, C. O., & Kaufman, Y. J. (2003). An enhanced contextual fire detection algorithm
677 for MODIS. *Remote Sensing of Environment*, 87(2–3), 273–282.
- 678 Gray, J., Sulla-Menashe, D., & Friedl, M. A. (2022). *User Guide to Collection 6.1 MODIS Land Cover Dynamics*
679 *(MCD12Q2) Product*.
- 680 Heinemann, A., Mertz, O., Frohling, S., Christensen, A. E., Hurni, K., Sedano, F., Chini, L. P., Sahajpal, R.,
681 Hansen, M., & Hurr, G. (2017). A global view of shifting cultivation: Recent, current, and future extent.
682 *PLoS ONE*, 12(9). <https://doi.org/10.1371/journal.pone.0184479>
- 683 Hersbach, H., Bell, B., Berrisford, P., Hirahara, S., Horányi, A., Muñoz-Sabater, J., Nicolas, J., Peubey, C., Radu,
684 R., Schepers, D., Simmons, A., Soci, C., Abdalla, S., Abellan, X., Balsamo, G., Bechtold, P., Biavati, G.,
685 Bidlot, J., Bonavita, M., ... Thépaut, J. N. (2020). The ERA5 global reanalysis. *Quarterly Journal of the*
686 *Royal Meteorological Society*, 146(730). <https://doi.org/10.1002/qj.3803>
- 687 Holden, Z. A., & Jolly, W. M. (2011). Modeling topographic influences on fuel moisture and fire danger in
688 complex terrain to improve wildland fire management decision support. *Forest Ecology and Management*,
689 262(12). <https://doi.org/10.1016/j.foreco.2011.08.002>
- 690 Hutto, R. L., Keane, R. E., Sherriff, R. L., Rota, C. T., Eby, L. A., & Saab, V. A. (2016). Toward a more
691 ecologically informed view of severe forest fires. *Ecosphere*, 7(2). <https://doi.org/10.1002/ecs2.1255>
- 692 *India State Forest Report 2021*. (2022).
- 693 ISFR. (2019). *Indian state of forests report, vol. II. Forest Survey of India*. (Ministry of Environment Forest and
694 Climate Change) Kaulagarh Road, P.O. IPE Dehradun - 248195.
- 695 Jones, M. W., Abatzoglou, J. T., Veraverbeke, S., Andela, N., Lasslop, G., Forkel, M., Smith, A. J. P., Burton, C.,
696 Betts, R. A., van der Werf, G. R., Sitch, S., Canadell, J. G., Santín, C., Kolden, C., Doerr, S. H., & Quéré, C.
697 Le. (2022). Global and Regional Trends and Drivers of Fire Under Climate Change. In *Reviews of*
698 *Geophysics* (Vol. 60, Number 3). <https://doi.org/10.1029/2020RG000726>
- 699 Júnior, J. S. S., Paulo, J. R., Mendes, J., Alves, D., Ribeiro, L. M., & Viegas, C. (2022). Automatic forest fire
700 danger rating calibration: Exploring clustering techniques for regionally customizable fire danger
701 classification. *Expert Systems with Applications*, 193. <https://doi.org/10.1016/j.eswa.2021.116380>
- 702 Kalogiannidis, S., Chatzitheodoridis, F., Kalfas, D., Patitsa, C., & Papagrigoriou, A. (2023). Socio-Psychological,
703 Economic and Environmental Effects of Forest Fires. *Fire*, 6(7). <https://doi.org/10.3390/fire6070280>
- 704 Kandlikar, M. (2000). The causes and consequences of particulate air pollution in urban India: A synthesis of the
705 science. *Annual Review of Energy and the Environment*, 25. <https://doi.org/10.1146/annurev.energy.25.1.629>
- 706 Li, L. M., Song, W. G., Ma, J., & Satoh, K. (2009). Artificial neural network approach for modeling the impact of
707 population density and weather parameters on forest fire risk. *International Journal of Wildland Fire*, 18(6).
708 <https://doi.org/10.1071/WF07136>
- 709 Mahto, S. S., & Mishra, V. (2019). Does ERA-5 Outperform Other Reanalysis Products for Hydrologic
710 Applications in India? *Journal of Geophysical Research: Atmospheres*, 124(16).
711 <https://doi.org/10.1029/2019JD031155>
- 712 Matt Jolly, W., Freeborn, P. H., Page, W. G., & Butler, B. W. (2019). Severe fire danger index: A forecastable
713 metric to inform firefighter and community wildfire risk management. *Fire*, 2(3).
714 <https://doi.org/10.3390/fire2030047>
- 715 McHugh, M. L. (2013). The chi-square test of independence. *Biochimica Medica*, 23(2), 143–149.
- 716 McNally, A., Arsenault, K., Kumar, S., Shukla, S., Peterson, P., Wang, S., Funk, C., Peters-Lidard, C. D., &
717 Verdin, J. P. (2017). A land data assimilation system for sub-Saharan Africa food and water security
718 applications. *Scientific Data*, 4. <https://doi.org/10.1038/sdata.2017.12>



- 719 Michael, Y., Helman, D., Glickman, O., Gabay, D., Brenner, S., & Lensky, I. M. (2021). Forecasting fire risk with
720 machine learning and dynamic information derived from satellite vegetation index time-series. *Science of the*
721 *Total Environment*, 764. <https://doi.org/10.1016/j.scitotenv.2020.142844>
- 722 Mitsopoulos, I., & Mallinis, G. (2017). A data-driven approach to assess large fire size generation in Greece.
723 *Natural Hazards*, 88(3). <https://doi.org/10.1007/s11069-017-2934-z>
- 724 Mohanty, A., & Mithal, V. (2022). Managing Forest Fires in a Changing Climate. *Council on Energy, Environment*
725 *and Water: New Delhi, India*. [https://www.ceew.in/sites/default/files/ceew-research-on-states-prone-to-forest-](https://www.ceew.in/sites/default/files/ceew-research-on-states-prone-to-forest-wildfires-india-and-mitigation-methods.pdf)
726 [wildfires-india-and-mitigation-methods.pdf](https://www.ceew.in/sites/default/files/ceew-research-on-states-prone-to-forest-wildfires-india-and-mitigation-methods.pdf)
- 727 Muñoz-Sabater, J., Dutra, E., Agustí-Panareda, A., Albergel, C., Arduini, G., Balsamo, G., Boussetta, S., Choulga,
728 M., Harrigan, S., Hersbach, H., Martens, B., Miralles, D., Piles, M., Rodríguez-Fernández, N., Zsoter, E.,
729 Buontempo, C., & Thépaut, J.-N. (2021). ERA5-Land: A state-of-the-art global reanalysis dataset for land
730 applications. *Earth System Science Data Discussions*. <https://doi.org/10.5194/essd-2021-82>
- 731 Nagendra, H., Paul, S., Pareeth, S., & Dutt, S. (2009). Landscapes of protection: Forest change and fragmentation
732 in Northern West Bengal, India. *Environmental Management*, 44(5). [https://doi.org/10.1007/s00267-009-](https://doi.org/10.1007/s00267-009-9374-9)
733 [9374-9](https://doi.org/10.1007/s00267-009-9374-9)
- 734 Naveh, Z. (1989). Fire in the Mediterranean - a Landscape Ecological Perspective. *Fire in Ecosystems Dynamics*.
- 735 Pausas, J. G., & Keeley, J. E. (2019). Wildfires as an ecosystem service. *Frontiers in Ecology and the Environment*,
736 17(5). <https://doi.org/10.1002/fee.2044>
- 737 Purcell, L. C. (2003). Comparison of thermal units derived from daily and hourly temperatures. *Crop Science*,
738 43(5). <https://doi.org/10.2135/cropsci2003.1874>
- 739 Quilcaille, Y., Batibemiz, F., Ribeiro, A. F. S., Padrón, R. S., & Seneviratne, S. I. (2023). Fire weather index data
740 under historical and shared socioeconomic pathway projections in the 6th phase of the Coupled Model
741 Intercomparison Project from 1850 to 2100. *Earth Syst. Sci. Data*, 000583391(15).
- 742 Reddy, C. S., Bird, N. G., Sreelakshmi, S., Manikandan, T. M., Asra, M., Krishna, P. H., Jha, C. S., Rao, P. V. N.,
743 & Diwakar, P. G. (2019). Identification and characterization of spatio-temporal hotspots of forest fires in
744 South Asia. *Environmental Monitoring and Assessment*, 191. <https://doi.org/10.1007/s10661-019-7695-6>
- 745 Reddy, C. S., Krishna, P. H., Anitha, K., & Joseph, S. (2012). Mapping and inventory of forest fires in Andhra
746 Pradesh, India: current status and conservation needs. *International Scholarly Research Notices*, 2012.
- 747 Reddy, C. S., Sreelekshmi, S., Jha, C. S., & Dadhwal, V. K. (2013). National assessment of forest fragmentation in
748 India: Landscape indices as measures of the effects of fragmentation and forest cover change. *Ecological*
749 *Engineering*, 60, 453–464.
- 750 Renard, Q., Pliissier, R., Ramesh, B. R., & Kodandapani, N. (2012). Environmental susceptibility model for
751 predicting forest fire occurrence in the Western Ghats of India. *International Journal of Wildland Fire*, 21(4).
752 <https://doi.org/10.1071/WF10109>
- 753 Roy, P. S., Behera, M. D., Murthy, M. S. R., Roy, A., Singh, S., & Kushwaha, S. P. S. (2015). ... & Ramachandran,
754 R. M. *New Vegetation Type Map of India Prepared Using Satellite Remote Sensing: Comparison with Global*
755 *Vegetation Maps and Utilities*, 39, 142–159.
- 756 Samiuddin, M., & El-Sayyad, G. M. (1990). On nonparametric kernel density estimates. *Biometrika*, 77(4), 865–
757 874.
- 758 Satir, O., Berberoglu, S., Akca, E., & Yeler, O. (2017). Mapping the dominant forest tree distribution using a
759 combined image classification approach in a complex Eastern Mediterranean basin. In *Journal of Spatial*
760 *Science* (Vol. 62, Number 1). <https://doi.org/10.1080/14498596.2016.1212414>
- 761 Scheper, A. C., Verweij, P. A., & van Kuijk, M. (2021). Post-fire forest restoration in the humid tropics: A
762 synthesis of available strategies and knowledge gaps for effective restoration. *Science of the Total*
763 *Environment*, 771. <https://doi.org/10.1016/j.scitotenv.2020.144647>
- 764 Silva, C. H. L., Aragão, L. E. O. C., Fonseca, M. G., Almeida, C. T., Vedovato, L. B., & Anderson, L. O. (2018).
765 Deforestation-induced fragmentation increases forest fire occurrence in central Brazilian Amazonia. *Forests*,
766 9(6). <https://doi.org/10.3390/f9060305>
- 767 Silva-Junior, C. H. L., Buna, A. T. M., Bezerra, D. S., Costa, O. S., Santos, A. L., Basson, L. O. D., Santos, A. L.
768 S., Alvarado, S. T., Almeida, C. T., Freire, A. T. G., Rousseau, G. X., Celentano, D., Silva, F. B., Pinheiro,
769 M. S. S., Amaral, S., Kampel, M., Vedovato, L. B., Anderson, L. O., & Aragão, L. E. O. C. (2022). Forest



770 Fragmentation and Fires in the Eastern Brazilian Amazon–Maranhão State, Brazil. *Fire*, 5(3).
771 <https://doi.org/10.3390/fire5030077>

772 Singh, R. D., Gumber, S., Tewari, P., & Singh, S. P. (2016). Nature of forest fires in Uttarakhand: Frequency, size
773 and seasonal patterns in relation to pre-monsoonal environment. *Current Science*, 111(2).
774 <https://doi.org/10.18520/cs/v111/i2/398-403>

775 Stocks, B. J., Lawson, B. D., Alexander, M. E., Wagner, C. V., McAlpine, R. S., Lynham, T. J., & Dube, D. E.
776 (1989). The Canadian forest fire danger rating system: an overview. *The Forestry Chronicle*, 65(6), 450–457.

777 Sudhakar Reddy, C., Jha, C. S., Manaswini, G., Alekhya, V. V. L. P., Vazeed Pasha, S., Satish, K. V., Diwakar, P.
778 G., & Dadhwal, V. K. (2017). Nationwide assessment of forest burnt area in India using Resourcesat-2
779 AWiFS data. *Current Science*, 112(7). <https://doi.org/10.18520/cs/v112/i07/1521-1532>

780 Taylor, S. W., & Alexander, M. E. (2006). Science, technology, and human factors in fire danger rating: The
781 Canadian experience. In *International Journal of Wildland Fire* (Vol. 15, Number 1).
782 <https://doi.org/10.1071/WF05021>

783 Tian, X., McRae, D. J., Jin, J., Shu, L., Zhao, F., & Wang, M. (2011). Wildfires and the Canadian Forest Fire
784 Weather Index system for the Daxing'anling region of China. *International Journal of Wildland Fire*, 20(8),
785 963–973.

786 Tripathi, O. P., Upadhaya, K., Tripathi, R. S., & Pandey, H. N. (2010). Diversity, Dominance and Population
787 Structure of Tree Species along Fragment-Size Gradient of a Subtropical Humid Forest of Northeast India.
788 *Research Journal of Environmental and Earth Sciences*, 2(2).

789 Tyukavina, A., Potapov, P., Hansen, M. C., Pickens, A. H., Stehman, S. V., Turubanova, S., Parker, D., Zalles, V.,
790 Lima, A., Kommareddy, I., Song, X. P., Wang, L., & Harris, N. (2022). Global Trends of Forest Loss Due to
791 Fire From 2001 to 2019. *Frontiers in Remote Sensing*, 3. <https://doi.org/10.3389/frsen.2022.825190>

792 Upton, G. J. (1992). Fisher's exact test. *Journal of the Royal Statistical Society: Series A (Statistics in Society)*,
793 155(3), 395–402.

794 Vadrevu, K. P., Eaturu, A., & Badarinath, K. V. S. (2010). Fire risk evaluation using multicriteria analysis-a case
795 study. *Environmental Monitoring and Assessment*, 166(1–4), 223–239. <https://doi.org/10.1007/S10661-009-0997-3/METRICS>

796

797 van Wees, D., van Der Werf, R., G., Randerson, J. T., Andela, N., Chen, Y., & Morton, D. C. (2021). The role of
798 fire in global forest loss dynamics. *Global Change Biology*, 27(11), 2377.

799 Vancutsem, C., Achard, F., Pekel, J. F., Vieilledent, G., Carboni, S., Simonetti, D., Gallego, J., Aragão, L. E. O. C.,
800 & Nasi, R. (2021). Long-term (1990–2019) monitoring of forest cover changes in the humid tropics. *Science*
801 *Advances*, 7(10). <https://doi.org/10.1126/sciadv.abe1603>

802 Vasilakos, C., Kalabokidis, K., Hatzopoulos, J., Kallos, G., & Matsinos, Y. (2007). Integrating new methods and
803 tools in fire danger rating. *International Journal of Wildland Fire*, 16(3). <https://doi.org/10.1071/WF05091>

804 Wagner, C. E. Van. (1987). Development and structure of the Canadian forest fire weather index system. In
805 *Forestry*. In Can. For. Serv.
806 <http://scholar.google.com/scholar?hl=en&btnG=Search&q=intitle:Development+and+Structure+of+the+Canadian+Forest+Fire+Weather+Index+System#0>

807

808 Yule, G. U. (1897). On the theory of correlation. *Journal of the Royal Statistical Society*, 60(4), 812–854.

809 Zackrisson, O., Nilsson, M.-C., & Wardle, D. A. (1996). Key Ecological Function of Charcoal from Wildfire in the
810 Boreal Forest. *Oikos*, 77(1). <https://doi.org/10.2307/3545580>

811

812

813

814

815